

Effect of Template Existence on the Textural Properties of Iron-based Catalyst for Fischer Tropsch Reaction

Papahtsara Sirikulbodee^{1,2,a}, Sabaithip Tungkamani^{*1,2,b}, Monrudee Phongksorn^{1,2,c},
Tanakorn Ratana^{1,2,d}, Thana Sornchamni^{3,e}

¹Department of Industrial Chemistry, King Mongkut's University of Technology North Bangkok, Bangkok, Thailand.

²Research and Development Center for Chemical Engineering Unit Operation and Catalyst Design (RCC), King Mongkut's University of Technology North Bangkok, Bangkok, Thailand.

³PTT Public Company Limited, Bangkok, Thailand.

Email: ^apapahtsara.s5277@gmail.com, ^bsbtt@kmutnb.ac.th, ^cmps@kmutnb.ac.th, ^dtanakornr@kmutnb.ac.th, ^ethana.s@pttplc.com

Abstract

Fischer Tropsch reaction is one of the interesting topic for renewable and clean energy. Polymerization of carbon monoxide or carbon dioxide with hydrogen over metal supported catalyst can produce long chain hydrocarbons. Synthetic liquid hydrocarbons are promising alternative to fossil fuels. This research work has been focused on the synthesis of Fe based catalyst for Fischer Tropsch reaction. Mesoporous silica (MS) support prepared by a precipitation method using two different washing solution, distilled water (DW) and acid in ethanol solution (ET), and different calcination temperature. Then, Fe/MS was prepared by an incipient wetness impregnation method. All of samples were systematically characterized using various physical and chemical techniques. TEM and XRD analysis were used to ensure that the cubic Ia3d mesostructure is stable after calcination. FTIR spectra are useful to ascertain the existence of template in the support. TPR studies were also used to understand the nature of Fe species and their reducibility. The results reveal that washing the support with distilled water and calcination at 550°C can efficiently remove the triblock copolymer templates. The existence of template in the support affects the textural properties of all catalyst investigated.

Keywords: Template, Fe based catalyst, Mesoporous silica, Fischer Tropsch reaction

1. INTRODUCTION

The basis for industrial hydrogenation of carbon monoxide to fuel-type of hydrocarbon compounds is credited to Franz Fischer and Hans Tropsch. Fischer Tropsch synthesis (FTS), which converts syngas

(CO+H₂) derived from coal, natural gas and other carbon-containing materials into hydrocarbon fuel. Nowadays, FTS has been dramatically paid attention due to a shortage of petroleum reserves and environmental restrictions[1]. All the group VIII elements show considerable high activity for FTS. Fe-based catalysts are widely used in FTS due to high activity for FTS reaction and low cost compared to Co or Ru. Moreover, Fe based catalyst exhibits high water-gas-shift (WGS) activity, thus Fe is superior for the conversion of low H₂/CO ratio syngas derived from coal or biomass[2]. According to the literature, catalytic activity, selectivity, attrition resistance and stability are mostly reliant on the support [3, 4]. However, Fe based catalyst is usually active in high loading content [5]. The efficiency of the catalyst is dependent on the density of active site. A high dispersion leads to an increase in number of catalytically active site [6]. In high temperature, Iron-based catalysts can agglomeration and sintering. The addition of structural promoters or supports into Fe-based catalysts to suppress the agglomeration of active phase and to improve the mechanical properties of catalysts is beneficial [3]. Mesoporous materials have a large surface area, large pore volume and narrow pore size distribution. Among the different mesoporous materials, mesoporous silica (MS) is interesting to be used as a support for metal supported catalyst. Mesoporous materials are normally synthesized by employing cationic surfactants as the template agent. The templates are often formed from neutral surfactant molecules. The ability of this special class of molecules, having a polar head and a long, non-polar hydrocarbon tail, is to form micelles in polar solvents by placing the water-repelling hydrocarbon tails together in the center of a sphere, or sometimes a cylinder, to avoid water contact. In some case, an aqueous solution of combination of triblock copolymer (Pluronic P123) and butanol are used for controlling the structure of the material [7]. However, to remove this type of surfactant such as calcination, in most cases the as-synthesized samples are calcined for the template removal in the presence of oxygen or air above 550°C [8]. Burning the organic templates for the template removal can lead to the presence of the local defects and the structure collapse or shrinkage. In this present work, the impregnation method was used to design Fe supported catalyst with high loading. Iron (III) nitrate, Fe(NO₃)₂·9H₂O, was used as precursors and MS material was used as the mesoporous support. Different calcination temperature for template removal and type of washing solution were established for investigation the effect of template existence on the textural properties of iron-based catalyst for Fischer Tropsch reaction.

2. Experimental

2.1 Catalyst preparation

Mesoporous silica (MS) support was synthesized by precipitation method using amphiphilic triblock copolymers (Pluronic P123) and butanol as template. It was added to distilled water and hydrochloric solution with stirring. After that, butanol solution was added at 35°C, followed by the addition of TEOS. The solution was stirred for 24 h and then transferred to an autoclave, sealed and aged for 24 h. The resulting white precipitate was washed and dried at various conditions. Powder of support was calcined, pelletized and sieved to have granule size of 355-710µm. Then, Fe/MS was prepared by the incipient wetness impregnation method. All of the samples were systematically characterized using various physical and chemical techniques.

2.2 Catalysts characterization

N₂ adsorption was carried out in a physisorption analyzer (Belsorp-mini, BEL) at -196°C to determine the BET surface area and pore size distribution of the samples. Before the measurements, the samples were

degassed at 350°C for 4 h. Pore size distribution was calculated by Barret-joyner-Haalender (BJH) method from the desorption.

FTIR spectroscopy was carried out using KBr disc technique using a Fourier transform infrared spectrometer (Nicolet 6700 and Perkin Elmer Spectrum 2000) in the range of 4000-400 cm^{-1} , with 15 scans and resolution of 4 cm^{-1} .

XRD pattern was obtained using a Bruker AXS D8 Discover. The diffractions were recorded at low scattering angles in the 2θ range of 0.5-60°.

H₂-TPR profiles were carried out in Belcat basic. 0.05 g catalyst was loaded in a U-type quartz tube reactor and ramped from 40°C to 900°C in 5% H₂/Ar at flow rate of 50 mL/min. The heating rate was maintained at 10°C/min.

H₂-TPD profiles were carried out with Belcat basic (BEL JAPAN, INC). The sample was reduced with pure H₂ at a temperature of 480°C for 15 h. The catalyst was subsequently flushed at the same temperature with Ar gas. After reduction, the sample was cooled to 50°C. After H₂ adsorption, the system was purged with Ar gas to remove physisorbed H₂. The H₂-TPD profile was monitored using TCD while the temperature was increased from room temperature to 800°C at a rate of 10°C/min.

TEM images were obtained from a JEOL JEM-2010 electron microscope. For TEM measurements, the samples were prepared by dispersing the powdered samples as slurry in ethanol, after which they were dispersed and dried on a on a holey carbon film on a copper grid.

3. Results and discussions

3.1 BET surface area

The BET surface area, pore volume and average pore diameter of MS and 20%Fe/MS materials are shown in Table 1. The isotherms are type IV which is typical for highly organized mesoporous materials. This result indicates that a significant decrease in the BET surface area was observed for the catalysts. It can be seen that the BET surface area of MS materials are 434-504 m^2/g and Fe/MS catalysts are 286-338 m^2/g , indicating deposition of iron inside pore.

Table 1. BET surface area, total pore volume and mean pore diameter of MS and 20%Fe/MS materials

	S_{BET} (m^2/g)	V_{T} (cm^3/g)	D_{p} (Å)	a_{o}^{a} (Å)	δ_{o} (Å)
MS (DW550)	434	0.60	55.3	245.6	240.1
MS (DW750)	504	0.58	46.2	234.9	188.7
MS (ET550)	500	0.60	47.7	245.6	197.9
MS (ET750)	437	0.62	56.4	225.1	168.7
20%Fe/MS (DW550)	307	0.42	54.9	-	-
20%Fe/MS (DW750)	286	0.33	45.4	-	-
20%Fe/MS (ET550)	338	0.36	42.3	-	-
20%Fe/MS (ET750)	315	0.41	52.1	-	-

^a Unit cell parameter estimated from the position of the (2 1 1) diffraction line ($a_{\text{o}} = \sqrt{6d_{211}}$).

^b Pore wall thickness ($\delta_{\text{o}} = a_{\text{o}} - D_{\text{p}}$).

Moreover, it can be found that total surface area, total pore volume and pore diameter of MS support materials are high than that obtained from catalyst, as shown in Table 1. These results indicate that the iron oxide is located inside the silica pores. On the other hand, the pore size distributions show only a limited decrease with the introduction of metal oxides. The different washing solutions result in producing different

BET surface area. Using hydrochloric in ethanol solution and low calcined temperature as the template removal fluid yields very high removal efficiency. The high calcined temperature decreases in BET surface area attributed to the partial collapse of the framework [9]. Ability to remove template by using hydrochloric in ethanol solution is similar to using distilled water. These results are also subsequently confirmed by FTIR characterization.

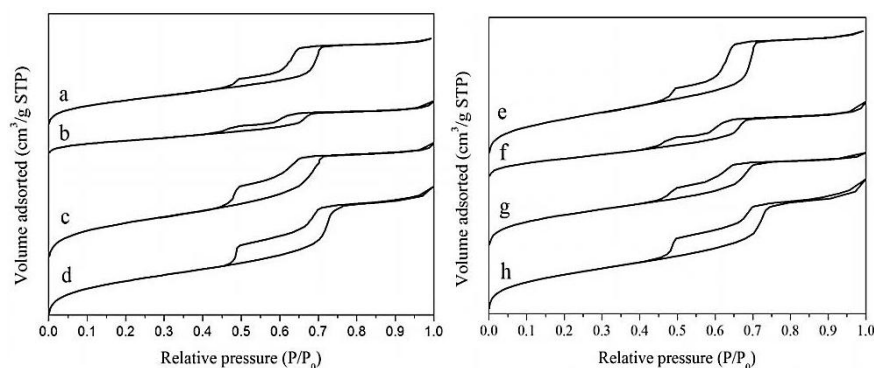


Figure 1. N₂ adsorption–desorption isotherms of (a) MS(ET750), (b) MS(ET550), (c) MS(DW750), (d) MS(DW550), (e) 20%Fe/MS(ET750), (f) 20%Fe/MS(ET550), (g) 20%Fe/MS(DW750) and (h) 20%Fe/MS(DW550)

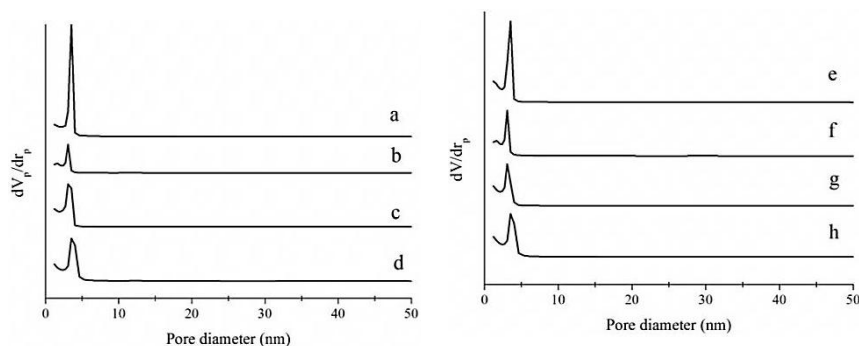


Figure 2. Pore size distribution of (a) MS(ET750), (b) MS(ET550), (c) MS(DW750), (d) MS(DW550), (e) 20%Fe/MS(ET750), (f) 20%Fe/MS(ET550), (g) 20%Fe/MS(DW750) and (h) 20%Fe/MS(DW550)

3.2 Fourier Transform Infrared Spectroscopy (FTIR)

Figure 3. shows FTIR spectra of 20%Fe/MS. The broad envelop around 3400 cm^{-1} is due to O–H stretching of surface hydroxyl groups, bridged hydroxyl groups and adsorbed water molecules, while deformational vibrations of adsorbed molecules cause the adsorption band at 1640 cm^{-1} . The presence of absorption bands around 2850 and 2975 cm^{-1} is corresponded to symmetric and asymmetric stretching vibrations of $-\text{CH}_2$ and $-\text{CH}_3$ groups, which belong to template remaining in the pores of the materials [10]. The corresponding bending mode was observed at 1380 cm^{-1} . The lower area of bands between 2850 and 2975 cm^{-1} confirms that calcination of the original framework was completed and that identity of the structure of template was completely disappeared from the calcined 20%Fe/MS catalyst. The bands between 450 and 1250 cm^{-1} are assigned to the framework vibrations of mesoporous silica materials. The asymmetric stretching vibrations of Si–O–Si and Si–O–Fe groups were observed between 950 and 1250 cm^{-1} and the corresponding symmetric stretching modes were obtained between 550 and 800 cm^{-1} . The band at 460 cm^{-1} is assigned to bending mode of Si–O–Si and Si–O–Fe bonds in their respective catalysts [10].

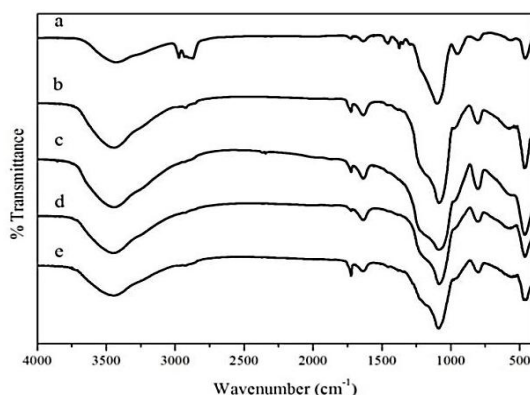


Figure 3. FT-IR spectra of (a) as-synthesized, (b) 20%Fe/MS(ET750), (c) 20%Fe/MS(ET550), (d) 20%Fe/MS(DW750) and (e) 20%Fe/MS(DW550)

3.3 X-Ray diffraction (XRD)

The XRD patterns of MS supports are shown in Figure 4. The low-angle powder XRD patterns MS materials reveal a well-developed and highly intense peak at $2\theta \approx 1^\circ$ corresponding to the plane (211) and a shoulder peak in the range $2\theta \approx 1.5\text{--}1.9^\circ$, assigned to a highly ordered cubic structure of the space group *Ia3d*. [2, 6, 11]. The interplanar spacing (d) was evaluated from the first peak corresponding to (211), then unit cell parameter (a_0) of 225.1, calculated from $a_0 = d_{211}\sqrt{6}$. The physicochemical properties of all calcined samples are given in Table 1. The wall thickness, calculated from the a_0 value of the XRD results and from the pore diameter, D_p , [6].

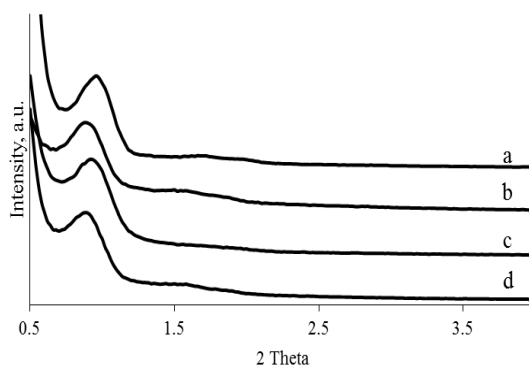


Figure 4. Low-angle XRD pattern of (a) MS(ET750), (b) MS(ET550), (c) MS(DW750) and (d) MS(DW550)

3.4 Hydrogen temperature programmed reduction with (H_2 -TPR)

H_2 -TPR profiles of all reduced samples containing 20 wt% Fe are shown in Figure 5. The profile presents at least three distinct peaks observed in a wide temperature interval. The lower temperature peak with well-defined maximum at 350°C is ascribed to the reduction of Fe_2O_3 to Fe_3O_4 . The overlapped peak between $450\text{--}550^\circ\text{C}$ is the reduction of Fe_2O_3 to FeO . The higher temperature peak around 600°C is belonged to the reduction of FeO to Fe^0 . This high temperature reduction could be due to the strong interaction of iron oxide with support. It has to be mentioned that at the same calcination temperature, the

reduction activity of catalyst washed by ET is better than DW. Moreover, at the same solvent, calcination temperature at 550°C is preferable.

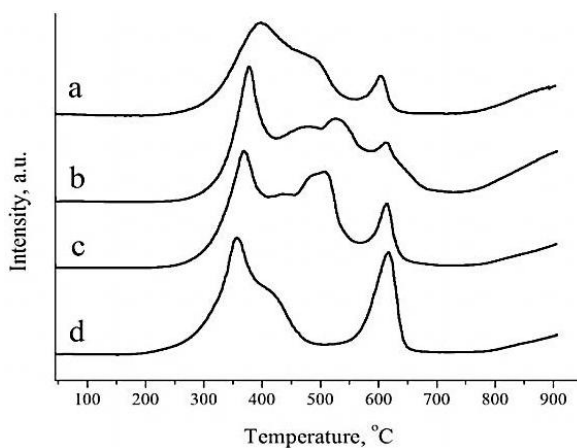


Figure 5. H₂-TPR profile of (a) 20%Fe/MS(DW750) (b) 20%Fe/MS(DW550), (c) 20%Fe/MS(ET750) and (d) 20%Fe/MS(ET550)

3.5 Hydrogen temperature programmed desorption (H₂-TPD)

H₂-TPD profiles of catalyst investigated are presented in Figure 7. H₂ desorption over MS supported catalysts mainly occurs in two broad temperature ranges: below 400°C and above 400°C. This indicates that H₂ desorbs from different active species. Less H₂ desorption was observed at lower temperature region, while most of desorbed H₂ was observed between 450-900°C. With increasing calcination temperature, the intensity of the second peak decreases and temperature maximum peak shifts from 700°C to high temperature. This suggests that the H₂ adsorption on surface iron sites is suppressed with calcination. According to the literature, H species desorbed below 200°C imply the attachment of hydrogen on weak adsorption sites of metallic iron surfaces. [12]. The results also show that 20%Fe/MS(DW550) catalyst give better desorption profile compared to other catalysts. This could be explained that the catalyst might have good metal dispersions. Thus 20%Fe/MS(DW550) catalyst was further investigated by TEM technique.

3.6 Transmission electron microscope (TEM)

TEM study was performed in order to analyze the mesoporous structure and dispersion of Fe on the support material. In Figure 7a-b., the TEM images present a nice channel structure of MS support. Calcination temperature does not affect the damage of support structure. On the other hand, calcination temperature has influence on the collapse of support structure with the presence of iron catalyst particles. TEM presented in Figure 7c-d. shows that the partial channel structure of MS support was collapsed. This could be ascribed by the high calcination temperature during preparation [13].

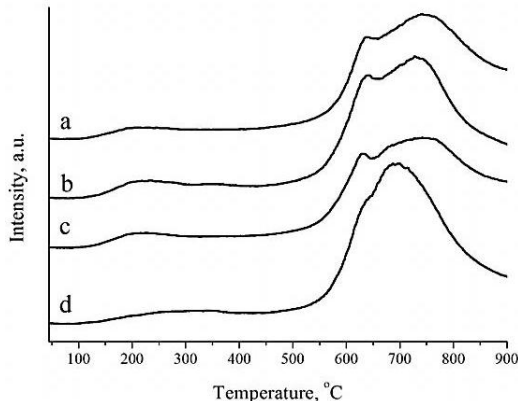


Figure 6. H₂-TPD profile of (a) 20%Fe/MS(ET750) (b) 20%Fe/MS(ET550), (c) 20%Fe/MS(DW750) and (d) 20%Fe/MS(DW550)

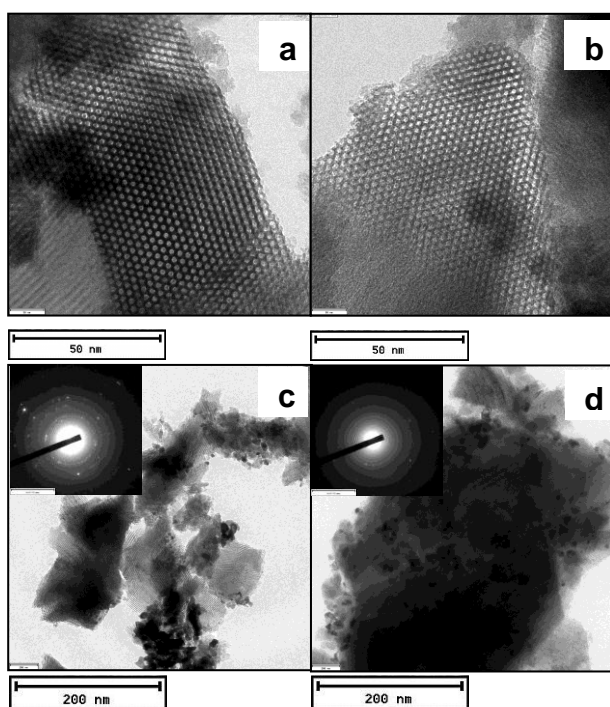


Figure 7. TEM image and Electron diffraction pattern of a) MS (DW550) and b) MS (DW750) c) 20%Fe/MS (DW550) and d) 20%Fe/MS (DW750)

4. Conclusions

This present work can be concluded that the existence of template in the support affects the textural properties of all catalyst synthesized. Washing the support with distilled water and calcination at 550°C can efficiently remove the triblock copolymer templates. Among catalyst investigated, 20%Fe/MS(DW550) presents a better physicochemical properties, which could be a result of high density of catalytically active sites and high dispersion confirmed by H₂-TPD and TEM analysis.

Acknowledgments

The authors would like to thank the Thailand Research Fund and PTT Public Company Limited (Research and Researchers for Industries – RRI: master degree, MSD56I0100) for financial support. Many thanks are due to National Science and Technology Development Agency, NSTDA, for assistance with obtaining the TEM.

References

- [1] Ali, S., N. Mohd Zabidi, et al., “Correlation between Fischer-Tropsch catalytic activity and composition of catalysts,” *Chemistry Central Journal*, Vol. 5, No. 68, pp. 1-8, 2011, Malaysia.
doi:10.1186/1752-153X-5-68
- [2] Lohitharn, N., J. G. Goodwin Jr, et al., “Fe-based Fischer–Tropsch synthesis catalysts containing carbide-forming transition metal promoters,” *Journal of Catalysis*, Vol. 255, No. 1, pp. 104-113, 2008, USA.
doi:10.1016/j.jcat.2008.01.026
- [3] Suo, H., S. Wang, et al., “Chemical and structural effects of silica in iron-based Fischer–Tropsch synthesis catalysts,” *Journal of Catalysis*, Vol. 286, pp. 111-123, 2012, China.
doi:10.1016/j.jcat.2011.10.024
- [4] Pour, A. N., M. R. Housaindokht, et al., “Fischer-Tropsch synthesis by nano-structured iron catalyst,” *Journal of Natural Gas Chemistry*, Vol. 19, No. 3, pp. 284-292, 2010, Iran.
doi:10.1016/S1003-9953(09)60059-1
- [5] Wan, H.-J., B.-S. Wu, et al., “Study of an iron-based Fischer–Tropsch synthesis catalyst incorporated with SiO₂,” *Journal of Molecular Catalysis A: Chemical*, Vol. 260, Issue1–2, pp. 255-263, 2006, China.
doi:10.1016/j.molcata.2006.07.062
- [6] Soni, K., B. S. Rana, et al., “3-D ordered mesoporous KIT-6 support for effective hydrodesulfurization catalysts,” *Applied Catalysis B: Environmental*, Vol. 90, No. 1–2, pp. 55-63, 2009, India.
doi:10.1016/j.apcatb.2009.02.010
- [7] Yue, W. and W. Zhou, “Crystalline mesoporous metal oxide,” *Progress in Natural Science*, Vol. 18, No. 11, pp. 1329-1338, 2008, United Kingdom.
doi:10.1016/j.pnsc.2008.05.010
- [8] Marcilla, A., M. Beltran, et al., “Template removal in MCM-41 type materials by solvent extraction: Influence of the treatment on the textural properties of the material and the effect on its behaviour as catalyst for reducing tobacco smoking toxicity,” *Chemical Engineering Research and Design*, Vol. 89, No. 11, pp. 2330-2343, 2011, Spain.
doi:10.1016/j.cherd.2011.04.015
- [9] Hao, Q., L. Bai, et al., “Activation pressure studies with an iron-based catalyst for slurry Fischer-Tropsch synthesis,” *Journal of Natural Gas Chemistry*, Vol. 18, No. 4, pp. 429-435, 2009, China.
doi:10.1016/S1003-9953(08)60134-6
- [10] Atchudan, R. and A. Pandurangan, “Growth of ordered multi-walled carbon nanotubes over mesoporous 3D cubic Zn/Fe-KIT-6 molecular sieves and its use in the fabrication of epoxy nanocomposites,” *Microporous and Mesoporous Materials*, Vol. 167, pp. 162-175, 2013, India.
doi:10.1016/j.micromeso.2012.08.031

- [11] Goscianska, J., A. Olejnik, et al., "In vitro release of l-phenylalanine from ordered mesoporous materials," *Microporous and Mesoporous Materials*, Vol. 177, pp. 32-36, 2013, Poland.
doi:10.1016/j.micromeso.2013.04.021
- [12] Li, J., C. Zhang, et al., "Effects of alkaline-earth metals on the structure, adsorption and catalytic behavior of iron-based Fischer–Tropsch synthesis catalysts," *Applied Catalysis A: General*, Vol. 464–465, pp. 10-19, 2013, China.
doi:10.1016/j.apcata.2013.04.042
- [13] Hussain, M., P. Akhter, et al., "Novel Ti-KIT-6 material for the photocatalytic reduction of carbon dioxide to methane," *Catalysis Communications*, Vol. 36, pp. 58-62, 2013, Italy.
doi:10.1016/j.catcom.2013.03.002